Molecular Structure of XeF_6. II. Internal Motion and Mean Geometry Deduced by Electron Diffraction*

L. S. BARTELL AND R. M. GAVIN, JR.†
Department of Chemistry, University of Michigan, Ann Arbor, Michigan

(Received 8 September 1967)

The distribution of internuclear distances in gaseous XeF_6 exhibits unusually diffuse XeF_6 bonded and F–F geminal nonbonded peaks, the latter of which is severely skewed. The distribution proves the molecule cannot be a regular octahedron vibrating in independent normal modes. The instantaneous molecular configurations encountered by the incident electrons are predominantly in the broad vicinity of C_{3v} structures conveniently described as distorted octahedra in which the xenon lone pair avoids the bonding pairs. In these distorted structures the XeF bond lengths are distributed over a range of approximately 0.08 Å with the longer bonds tending to be those adjacent to the avoided region of the coordination sphere. Fluorines suffer angular displacements from octahedral sites which range up to 5° or 10° in the vicinity of the avoided region.

Alternative interpretations of the diffraction data are developed in detail, ranging from models of statically deformed molecules to those of dynamically inverting molecules. In all cases it is necessary to assume that t_{1u} bending amplitudes are enormous and correlated in a certain way with substantial t_{2g} deformations. Notwithstanding the small fraction of time that XeF. spends near O_h symmetry, it is possible to construct a molecular potential-energy function more or less compatiable with the diffraction data in which the minimum energy occurs at O_h symmerty. The most notable feature of this model is the almost vanishing restoring force for small t_{1u} bending distortions. Indeed, the mean curvature of the potential surface for this model corresponds to a ν_4 force constant F_{44} of 10^{-2} mdyn/Å or less. Various rapidly inverting non-O_h structures embodying particular combinations of t_{2g} and t_{1u} deformations from O_h symmetry give slightly better radial distribution functions, however. In the region of molecular configuration where the gas molecules spend most of their time, the form of the potential-energy function required to represent the data does not distinguish between a Jahn–Teller first-order term or a cubic V_{445} term as the agent responsible for introducing the t_{2g} deformation. The Jahn–Teller term is consistent with Goodman's interpretation of the molecule. On the other hand, the cubic term is found to be exactly analogous to that for other molecules with stereochemically active lone pairs (e.g., SF_4, ClF_3). Therefore, the question as to why the XeF_6 molecule is distorted remains open. The reported absence of any observable gas-phase paramagnetism weighs against the Jahn–Teller interpretation.

The qualitative success but quantitative failure of the valence-shell–electron-pair-repulsion theory is discussed and the relevance of the "pseudo-Jahn–Teller" formalism of Longuet-Higgins *et al.* is pointed out. Brief comparisons are made with isoelectronic ions.

I. INTRODUCTION

The aura of novelty surrounding noble-gas compounds at the time of their discovery has faded rapidly in the face of the intense scrutiny to which the compounds have been subjected. The molecules have been found to possess chemical bonds closely related to those in long familiar substances.[1–3] One of the compounds, however, has lost little of its reputation as an oddity since its discovery in 1962. Xenon hexafluoride differs conspicuously in its properties from all of the other known hexafluorides.[4] It stubbornly resisted structural elucidation up to the time of the present study, and still poses unsolved questions.

It does not conform to the pattern of fairly rigid linear, symmetrical F–Xe–F bond configurations exhibited by XeF_2 and XeF_4 and forecast for XeF_6 by proponents of the three-center four-electron MO bonding picture.[1] Neither does it conform in detail to the rival Gillespie–Nyholm–Sidgwick–Powell theory[5–7] which predicts a severe distortion from O_h symmetry. Instead, it has intermediate properties and manifests its ambivalence by executing a triply degenerate vibration of enormous amplitude which is remarkable in its own right.

The body of electron-diffraction data presented in Paper I[8] do not in themselves provide sufficiently complete information to elucidate all molecular details of interest. The present paper examines alternative interpretations of the data in some detail. A certain amount of speculation is advanced in the hope that it will direct attention to potentially fruitful areas of research and stimulate experiments to establish more quantitatively the parameters of the molecular force field. Both the importance of the molecule's role in an unsettled area of valence theory and the novelty of its molecular dynamics would seem to justify this approach and to warrant a much more extensive discussion of the analysis than is customarily reported. The principal conclusions which may be drawn from the available data, diffraction and otherwise, are summarized in the final section.

* This research was supported by a grant from the National Science Foundation.

† Present address: Department of Chemistry, Haverford College, Haverford, Pa. 19041.

[1] See, for example, the discussions in *Noble Gas Compounds*, H. H. Hyman, Ed. (University of Chicago Press, Chicago, Ill., 1963), and the references therein.

[2] J. G. Malm, H. Selig, J. Jortner, and S. A. Rice, Chem. Rev. **65**, 199 (1965).

[3] H. H. Claassen, *The Noble Gases* (D. C. Heath and Co., Boston, Mass., 1966).

[4] B. Weinstock, Chem. Eng. News **42**, 86 (1964).

[5] N. V. Sidgwick and H. M. Powell, Proc. Roy. Soc. (London) **A176**, 153 (1940).

[6] R. J. Gillespie and R. S. Nyholm, Quart. Rev. (London) **11**, 339 (1957).

[7] R. J. Gillespie, J. Chem. Educ. **40**, 295 (1963).

[8] R. M. Gavin, Jr., and L. S. Bartell, J. Chem. Phys. **48**, 2460 (1968) (preceding article).

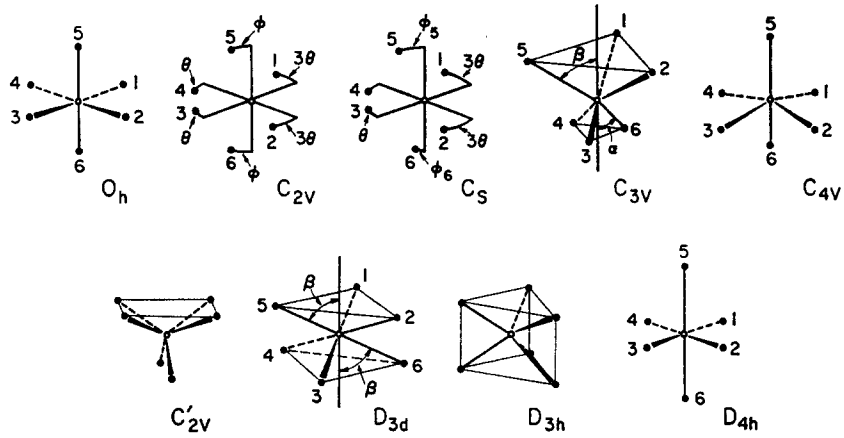

FIG. 1. Identification of models tested in XeF_6 structure analysis. See Table I for constraints imposed.

II. ANALYSIS IN TERMS OF A SINGLE STRUCTURAL CONFIGURATION

A. Tests of Various Structural Models

The molecular geometries receiving greatest attention in this phase of structure analysis are illustrated in Fig. 1 and described in Table I. An excellent representation of diffracted intensities can be obtained with a model possessing no elements of symmetry at all but, with such a large number of freely variable parameters, no unique solution is possible from the diffraction data alone. Therefore, it seems best in this phase of analysis to follow the usual criterion of simplicity adopted in electron-diffraction studies of complex molecules, namely, to favor the simplest model which will represent the data adequately.

As discussed below, the single configuration meeting this criterion most closely seems to be one with C_{2v} symmetry. The most general C_{2v} model would have six geometric and 10 vibrational amplitude parameters. While this is many fewer than for an unsymmetrical model, it is still too many to be derived definitely from the diffraction data, particularly since the electron phase shift parameter s_c[8] must also be determined empirically. Therefore (in all but a few tests) the following simplifying assumptions were adopted. It was assumed that at most two different XeF bond lengths occur in the molecule. Only two independent bond angle parameters were allowed to vary freely. The amplitudes associated with the two different bond lengths were allowed to vary independently but amplitudes of the nonbonded F–F peaks were lumped arbitrarily into three independent groups corresponding to shorter, middle, and longer distances. The breakdown for certain models is shown in Table II.

Of the models listed in Table I, those with conventional O_h, D_{3h}, D_{4h}, C_{2v}', and C_{4v} structures were unsatisfactory in representing the data. The O_h model was tested for obvious reasons and its unsatisfactory features have been discussed in Paper I.[3]

A trigonal prism with D_{3h} symmetry was discarded because it does not have the approximately linear F–Xe–F configuration needed to account for the 3.7-A F–F peak in the $f(r)$ function. Somewhat similar deficiencies weighed against the C_{2v}' model.

The model D_{4h} was investigated because it placed high in an informal poll of inorganic chemists who were asked to speculate about XeF_6. It can be ruled out because of its inability to move the intermediate peak enough without splitting the XeF peak excessively,

TABLE I. Models tested in XeF_6 structure analysis.[a]

Symmetry	XeF bond classes	Constraints on angles
O_h	All bonds equal	
C_{2v}	(a) F_1, F_2, F_3, F_4 long	$\theta=\phi$
	(b) F_1, F_2, F_3, F_4 long	$\theta\neq\phi$ (Model A)
	(c) F_5, F_6 long	$\theta=\phi$
	(d) F_1, F_3 long	$\theta=\phi$
	(e) All bonds equal	$\theta=\phi$
C_s	(a) F_1, F_2, F_3, F_4 long	$\phi_5\neq0$, $\phi_6=0$ (Model B)
	(b) F_5, F_6 long	$\phi_5\neq0$, $\phi_6=0$
	(c) F_1, F_2, F_5 long	$\phi_5=\phi_6\neq0$
C_{3v}	(a) F_1, F_2, F_5 long	$\beta>\alpha$ (Model C)
	(b) F_1, F_2, F_5 long	$\beta=\alpha$
	(c) F_1, F_2, F_5 long	$\beta<\alpha$
	(d) All bonds equal	
C_{4v}	various	various
C_{2v}'	various	various
D_{3d}	All bonds equal	$F_1XeF_3=F_2XeF_4$ $=F_5XeF_6$ $=180°$
D_{3h}	All bonds equal	various
D_{4h}	(a) F_5, F_6 long	90° or 180°
	(b) F_1, F_2, F_3, F_4 long	90° or 180°
Mixtures	(a) O_h plus D_{3d}	
	(b) Distribution along O_h to C_{3v} path	
	(c) Distribution along O_h to C_{2v} path	
	(d) Distribution along C_{3v} to C_{2v} path	
Models of facile inversion (see Sec. III of text)		

[a] In each model, unless otherwise noted, the various XeF bond lengths were constrained to assume one of at most two independent values. See Fig. 1 for notation.

TABLE II. XeF_6 structural parameters derived from experimental radial distribution function.[a]

	Model A C_{2v} Symmetry				Model B C_s Symmetry		Model C C_{3v} Symmetry			
	Analysis I[b]		Analysis II[b]		Analysis I		Analysis I		Analysis II	
$\sigma(f)$	0.0471		0.0526		0.0470		0.0503		0.0536	
r_{XeF}[c]	1.886±0.005		1.887±0.005		1.886±0.005		1.887±0.005		1.887±0.005	
Δr_{XeF}[d]	0.083±0.03		0.087±0.03		0.091±0.03		0.050±0.03		0.077±0.03	
$\Delta_{F_1XeF_4}$	81.9°		82.6°		81.6°		F_1XeF_2 100.6°		99.9°	
$\Delta_{F_5XeF_6}$	170°		168°		173°		F_3XeF_4 91.0°		91.0°	
dist	r_g	l_α	r_g	l_α	r_g	l_α	r_g	l_α	r_g	l_α
XeF_6	1.831	0.082	1.826	0.071	1.825	0.079	1.862	0.085	1.848	0.068
XeF_1	1.914	0.062	1.916	0.051	1.916	0.059	1.912	0.065	1.926	0.048
1–4	2.506	0.098	2.526	0.116	2.500	0.093	2.525	0.092	2.507	0.118
3–4		(same as 1–4)			(same as 1–4)		2.652	0.092	2.617	0.118
3–5	2.557	0.098	2.540	0.116	2.516	0.093	(same as 1–4)			
3–6		(same as 3–5)			2.644	0.093	(same as 3–4)			
1–5	2.708	0.133	2.722	0.151	2.644	0.128	2.939	0.277	2.828	0.272
1–6		(same as 1–5)			2.730	0.128	(same as 1–4)			
1–2	3.212	0.133	3.178	0.151	3.232	0.128	(same as 1–5)			
5–6	3.644	0.052	3.636	0.060	3.640	0.052	3.765	0.070	3.758	0.070
1–3	3.787	0.052	3.799	0.060	3.787	0.052	(same as 5–6)			

Assumed shrinkage corrections for nonbonded distances 0.002–0.003 Å

[a] See Fig. 1 and Table I for numbering scheme and imposed constraints.
[b] See Footnote 9.
[c] A slightly higher mean bond length of 1.890±0.005 Å, as derived by placing lower weight on data at small scattering angles, seems preferable. See text.
[d] Difference in length between the two assumed classes of bonds. See Table I.

among other reasons. Of the models in the above listing, the C_{4v} model showed some features consistent with the observed radial distribution curve. Nevertheless, it required seemingly excessive amplitudes of vibration for the four distances splitting outward from the 2.7-Å peak.

Simple models which were reasonably consistent with the diffraction data are given in Table II together with values of their parameters derived from least-squares fits of the experimental data. They are designated as A (C_{2v} symmetry), B (C_s symmetry), and C (C_{3v} symmetry). Their physical characteristics and interpretation will be discussed in the next section. Models A and B are very similar except for the lower symmetry of B. Although our criterion of simplicity favors the model with higher symmetry, it seems worthwhile to list B to show the effect on the least-squares parameters derived when the imposed symmetry, restrictions are varied. In Models A and B the additional restriction has been introduced, although not required by the symmetry, that the shorter nonbonded equatorial distances F_1–F_4, F_2–F_3, and F_3–F_4 are equal. This simplification, which was imposed to make the analysis more tractable, is physically plausible for the packing of ligands. Strengthening this argument is the fact that in Model A the least-squares fitting makes the other close backside contacts F_3–F_5 etc., essentially the same length as the equatorial contacts F_1–F_4 etc., even though the F_1–F_4 and F_3–F_5 distances are varied independently.

In model C the higher C_{3v} symmetry made it possible to vary all geometric variables freely with no further restrictions since there are only four independent parameters. In analysis I (adopting standard electron scattering approximations)[9] it became evident that the amplitude of the F_1–F_2 and equivalent peak did not converge to a definite value but tended to increase beyond what we, at that time, regarded as physical reasonability. For the purposes of listing least-squares parameters of some physical plausibility in Table II, we imposed the constraint for model C that its F_1–F_2 and equivalent amplitudes were not to exceed the other F–F amplitudes by more than 0.185 Å. In Analysis II (based on more exact scattering expressions)[9] the F_1–F_2 mean amplitude derived was large but the parameter did converge in radial distribution analysis. It did not converge properly in fits of the intensity function over the individual ranges covered in a given camera geometry.

Some interesting conjectures of Goodman[10] to be discussed in a later section led to the test of D_{3d} sym-

[9] In Analysis I Hartree–Fock x-ray elastic scattering factors and Heisenberg–Bewilogua inelastic scattering factors were employed. Corrections for the failure of the Born approximation were made only through the use of the Thomas–Fermi phase shifts of Hoerni and Ibers rescaled in effective atomic number to fit the experimental data.

In Analysis II elastic scattering was based on the new partial wave calculations of Cox and Bonham (H. L. Cox, Doctoral dissertation, Indiana University, 1967). Hartree–Fock inelastic scattering factors for F [C. Tavard, D. Nicholas, and M. Roualt, J. Chim. Phys. **64**, 540 (1967)] and for Xe [extrapolated from the iodine factors of R. F. Pohler and H. P. Hansen, J. Chem. Phys. **42**, 2347 (1965)] were used.

[10] G. Goodman, Bull. Am. Phys. Soc. **12**, 296 (1967).

metry. The diffraction data are not in satisfactory accord with a D_{3d} model unless a rather remarkable vibrational mode with large amplitudes of oscillation is considered. Goodman's suggestion was that the vapor may consist of a mixture of singlet O_h and triplet D_{3d} molecules. The pattern of such a mixture would be characterized by four parameters: the composition, the O_h bond length, and the D_{3d} bond length and angle of distortion from O_h. A combination of the four parameters can be found which minimizes the misfit with the data. This combination (Analysis I)[6] with about one O_h molecule ($r_{XeF}=1.84$ Å) for every two D_{3d} molecules ($r_{XeF}=1.91$ Å, $\beta\approx 60.0°$) is distinctly inferior to the best C_{2v} and C_{3v} models, however, if reasonably normal amplitudes of vibration are assumed. Any fairly close fit of the O_h, D_{3d} mixture turns out to be obtained by assigning such an enormous amplitude of vibration to the F_1–F_2 (and equivalent) distances that the peak height is small and the peak area spills out to large r values.

A closer inspection of a vibrational mechanism which would preferentially broaden only one of the two geminal F–F peaks for a D_{3d} molecule reveals that the vibrational mode would have to be an ungerade mode (a_{2u}) of exceedingly low restoring force. Of special interest is the fact that this mode corresponds to an oscillation carrying a C_{3v} structure very closely related to that discussed above on through a D_{3d} intermediate into a mirror image of the initial C_{3v} configuration. Such a "D_{3d}" molecule would, accordingly, be deformed far into a C_{3v} geometry on the average. It is possible, therefore, to construct a "D_{3d}" model embodying sizeable a_{2u} oscillations which gives a reasonably good fit with the diffraction data even if the concentration of O_h molecules is set equal to zero.

We may conclude then, that the diffraction data provide no evidence that normal O_h molecules are present. If we must choose a *single molecular configuration* to account for the experimental observations we must select a structure closely related to the C_{2v} or C_{3v} models in Table II, as discussed above. Ordinarily, the C_{2v} structure would be given greater credence because it gives the closest fit with the least abnormal amplitudes of vibration.

B. Uncertainties

Physically meaningful uncertainties are difficult enough to determine for parameters of simple molecules, and even more difficult for XeF_6 in view of the added constraints and simplifications. Therefore, the values given in Table II are to be taken only as rough guides of standard errors. The most accurate structural parameter is the mean bond length r_g of the composite XeF peak for which the standard error is listed as ± 0.005 Å. Mean amplitudes of the two assumed components of the XeF peak, and Δr_{XeF}, the difference between the two components, have standard errors of approximately 0.02 and 0.03 Å, respectively. A significant contributor to this uncertainty is the uncertainty of ± 0.8 Å^{-1} in the Born phase reversal parameter s_c.[8] Neglected in this and in the other uncertainties listed in Table II is the possible influence of the restrictions imposed in the analyses. An additional small source of error may stem from the shrinkage corrections δr adopted in the analysis and listed in Table II. These corrections are rough estimates made from shrinkage values for octahedral molecules calculated by Meisingseth and Cyvin.[11] The estimates are very crude indeed, if not altogether meaningless, since the XeF_6 motions are quite different from those of the comparison molecules.

A troublesome feature which interfered appreciably with the analysis of positions and breadths of individual XeF component peaks in the composite is the pronounced foot on the leading edge of the principal peak. No reasonable refinements of the background curve could eliminate this foot. Since the foot is larger than our usual error signals in the case of lighter atoms, and since somewhat analogous feet have been encountered in our recent work on other xenon and iodine compounds, it is possible that the feature signifies an inadequately understood aspect of electron scattering theory. The anomalous range of intensity data contributing to the "foot" is mainly inside $s=10$ Å^{-1}, with the largest contribution from s values lower than 6. This region is particularly sensitive to assumptions about the electron distribution in the molecule. Because of the shape of this anomaly in the $f(r)$ peak it is not unexpected to find that the mean Xe–F bond length derived from the intensity data varies slightly depending upon the data range included. Least-squares fits of r^2 sector data (camera range $2<s<10$) gave 1.881 ± 0.0014 Å, fits of r^3 sector data (camera range $5<s<20$) gave 1.893 ± 0.0012 Å, and fits of r^3 sector data (camera range $15<2<40$) gave 1.894×0.008 Å. Obviously the standard errors derived from curve fitting do not take into account important sources of uncertainty. Similar shifts in the indicated bond length from camera range to camera range were reported for TeF_6 by Seip and Stoelevik.[12] Our best judgement places the weighted average r_{XeF} at about 1.890 ± 0.005 Å.

C. Discussion of Molecular Parameters

The diffraction data clearly show that the average configuration of XeF_6 departs appreciably from O_h symmetry. They also show, however, that the structure is essentially a distorted octahedron rather than, say, a trigonal prism, since the long F–F distance is nearly twice the mean XeF bond length. The more successful models all have the common feature that the fluorines tend to avoid a certain point on the coordination sphere and migrate toward the other side of the molecule. In order to advance a convenient picture to aid in the visualization of the deformations involved,

[11] E. Meisingseth and S. J. Cyvin, Acta Chem. Scand. **16**, 2452 (1963).

[12] H. M. Seip and R. Stoelevik, Acta Chem. Scand. **20**, 1535 (1966).

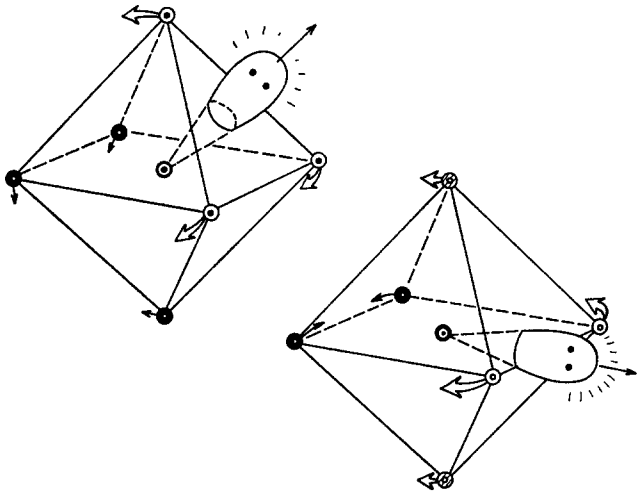

FIG. 2. Schematic representation of deformations consistent with diffraction patterns. The influence of xenon's lone pair according to the valence-shell-electron-pair-repulsion theory is portrayed.

and for sake of brevity in descriptions of structures, we shall refer to the avoided region on the coordination sphere as the Gillespie lone pair of electrons.[6,7,13,14] If we start with an undeformed octahedron we can characterize the deformation to the equilibrium structure in terms of the site of the repulsive lone pair, as suggested in Fig. 2. The lone pair may be directed toward a corner, a face, or an edge of the octahedron. Symmetry considerations would seem to dictate that the lone pair be *centered* on the corner, face, or edge in the equilibrium structure. If the lone pair is directed toward a corner of the octahedron, the corner atom is presumably pushed outward slightly while the four adjacent ligands are repelled towards the opposite corner, leading to a C_{4v} structure. In this deformation *four adjacent F–F distances increase*, four are nearly unchanged, and four decrease. Similarly, if the lone pair protrudes through the center of a face, a C_{3v} structure results in which *three adjacent F–F distances increase* and nine tend to decrease. If the lone pair points toward an edge a C_{2v} configuration is induced in which *one* F–F *nonbonded distance is increased sharply*, four are changed only modestly, and seven tend to decrease. The order of structure preference $C_{2v} > C_{3v} > C_{4v}$ in interpretation of the diffraction data stems largely from the smallness of area in the radial distribution curve corresponding to adjacent F–F distances greater than the O_h reference edge length. It is interesting to note that the C_{2v} structure is a distorted pentagonal bipyramid with a vacant equatorial site. According to Gillespie's model,[7,13] XeF_6 should correspond to a seven-coordinated structure and exhibit some similarities to IF_7. Iodine heptafluoride is itself a pentagonal bipyramid.[15]

Bond lengths and amplitudes of vibration provide additional clues for interpreting the bonding in XeF_6. The mean length of bonds in XeF_6 is 1.890 Å, consistent with the trend set by $XeOF_4$, XeF_4, and XeF_2 with bond lengths of 1.90±0.01 Å,[16] 1.95±0.01 Å,[17] and 2.00±0.01 Å,[18] respectively. Even the longer of the XeF_6 bonds (at 1.92_6 Å) are shorter than the XeF_4 bonds. Infrared XeF stretching frequencies for XeF_2, XeF_4, and $XeOF_4$ are 555, 586, and 608 cm^{-1}, respectively,[1–3] and a strong absorption[1–3] for XeF_6 at 612 cm^{-1} seems to confirm the trend of XeF bond tightening as electronegative atoms are added to the xenon.[1–3] Therefore, it is reasonable to expect that the Xe–F bond stretching force constant *increases* in the series XeF_2, XeF_4, XeF_6 and that the intrinsic amplitude of vibration of an XeF bond *decreases*. Nagarajan[19,20] has calculated that the root-mean-square stretching amplitudes for XeF_2 and XeF_4 are 0.0435 and 0.0429 Å at 0°K, and 0.0474 and 0.0475 Å at 298°K. These values are similar to those found for the closely analogous bonds in IF_7[15] and for all other hexafluorides[21–23] and must, accordingly, be considered as reliable references to apply to XeF_6.

In apparent disagreement with this conclusion are the experimental amplitudes of about 0.07_5 and 0.05_5 A listed for the shorter and longer bond components of XeF_6 in Table II. This disagreement and seeming

[13] R. J. Gillespie, Ref. 1, p. 333.
[14] R. J. Gillespie, Alfred Werner Centennial Symposium, American Chemical Society Meeting, New York, September 1966.
[15] H. B. Thompson and L. S. Bartell, Trans. Am. Cryst. Assoc. **2**, 190 (1966); H. B. Thompson, W. Adams, L. Winstrom, and L. S. Bartell (unpublished).
[16] E. J. Jacob, H. B. Thompson, and L. S. Bartell, J. Chem. Phys. **47**, 3736 (1967).
[17] D. H. Templeton, A. Zalkin, J. D. Forrester, and S. M. Williamson, J. Am. Chem. Soc. **85**, 242 (1963); J. A. Ibers and W. C. Hamilton, Science **139**, 106 (1963); J. H. Burns, P. A. Agron, and H. A. Levy, *ibid.* **139**, 1208 (1963); R. K. Bohn, K. Katada, J. V. Martinez, and S. H. Bauer, Ref. 1, p. 238.
[18] S. Siegel and E. Gebert, J. Am. Chem. Soc. **85**, 240 (1963); H. A. Levy and P. A. Agron, *ibid.* **85**, 241 (1963).
[19] G. Nagarajan (private communication).
[20] G. Nagarajan, Acta Phys. Austriaca **18**, 11 (1964). Note, however, that the force constants were based on an incorrect assignment of the e_u bending mode.
[21] M. Kimura, V. Schomaker, D. Smith, and B. Weinstock (unpublished).
[22] H. M. Seip, Acta Chem. Scand. **19**, 1955 (1965); H. M. Seip and R. Stoelevik, *ibid.* **20**, 1535 (1966); H. M. Seip and R. Seip, *ibid.* **20**, 2698 (1966).
[23] E. Meisingseth and S. J. Cyvin, Acta Chem. Scand. **16**, 2452 (1962); M. Kimura and K. Kimura J. Mol. Spectry. **11**, 368 (1963).

anomaly[24] that the shorter bond has the greater amplitude may be taken as evidence that the components we have resolved (in restricting bond lengths to two classes) are in reality composites themselves. A C_{2v} molecule has three rather than two nonequivalent bonds. Furthermore, evidence to be discussed in the next sections suggests that the molecule inverts rather freely, thereby going through intermediate configurations exhibiting a distribution of bond types.

III. ANALYSIS IN TERMS OF MOLECULAR INVERSION

A. Preliminary Considerations

The distortion of the best single structural configurations from O_h symmetry is curiously small—quite a bit smaller than predicted by Gillespie's rules[7]—and only somewhat greater than the apparent amplitudes of vibration. This circumstance demands that models of dynamic inversion be considered as well as the models of static deformation so far considered.

Preliminary tests with distributions of configurations soon confirmed (1) that it was not helpful to consider more than a small concentration of O_h configurations and (2) that in tests for which all skeletal amplitudes were taken to be normal except those of the inversion mode, far better fits were obtained when the distribution corresponded to a lone pair sampling face and edge sites than to a localized lone pair.

The picture of facile inversion can account for the absence of an observable dipole moment in a recent molecular-beam experiment by Falconer *et al.*[25] It can also help to explain the "unusual band contours and abnormally great breadth" of the infrared bands noted by Smith.[26] Other supporting evidence for the freedom of internal motion of the molecule is provided by the entropy data, according to arguments by Weinstock *et al.*[27]

The above considerations provide ample justification for investigating the internal motion of a nominally octahedral molecule in greater detail. This is best initiated by examining the symmetry coordinates and normal coordinates of octahedral molecules.

B. Remarks About Normal Coordinates

For molecules undergoing infinitesimal amplitudes of vibration it can be shown that vibrational motions consist of superpositions of normal modes each of which has a characteristic frequency. Even when too little is known about the potential function to establish the normal coordinates for a molecule, many simplifications result if the symmetry coordinates are considered instead of the simple internal coordinates.[28] Since we will have many occasions to refer to the symmetry coordinates of octahedral molecules[29] we illustrate them in Fig. 3. According to normal-coordinate theory, vibrational motions of one symmetry class are absolutely uncorrelated with motions of another symmetry. We shall see that the present electron-diffraction intensities cannot be explained on the basis of an O_h molecule vibrating in independent normal modes.

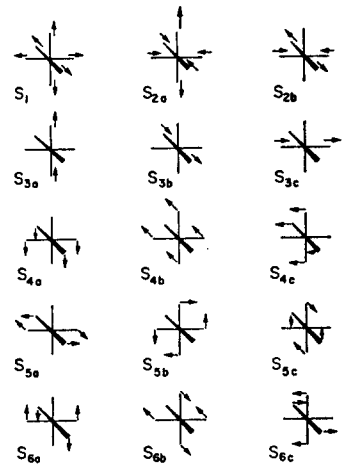

FIG. 3. Symmetry coordinates for O_h reference configuration.

C. Molecular Displacements Required by Diffraction Data

It is a simple matter to deduce the spectrum of internuclear distances in XeF_6 corresponding to a given static deformation from O_h symmetry along some particular symmetry coordinate. For small deformations along any t_{1u}, t_{2g}, or t_{2u} coordinate the three peaks at r_{XeF}, $2^{1/2}r_{XeF}$, and $2r_{XeF}$ are each either unchanged or split symmetrically into subpeaks. Static deformations along e_g coordinates can split the peaks unsymmetrically. Even for these deformations, however, a change of the sign of the e_g coordinates mirrors the subpeaks about the O_h reference peak center. It is evident, then, that harmonic oscillations along any particular symmetry coordinate will have the effect of broadening the peaks centered at r_{XeF}, $2^{1/2}r_{XeF}$, and $2r_{XeF}$, but will not displace them (except for very minor "shrinkage effects")[30] or skew them. If the modes of different symmetry are uncorrelated in phase, any distribution

[24] The anomaly may be an artifact of the "foot" on the leading edge of the XeF peak.

[25] W. E. Falconer, A. Büchler, J. L. Stauffer, and W. Klemperer, "Molecular Structure of XeF_6 and IF_7," J. Chem. Phys. (to be published).

[26] D. F. Smith, Ref. 1, p. 295.

[27] B. Weinstock, E. E. Weaver, and C. P. Knop, Inorg. Chem. **5**, 2189 (1966); B. Weinstock (private communication).

[28] E. B. Wilson, Jr., J. C. Decius, and P. C. Cross, *Molecular Vibrations* (McGraw-Hill Book Co., New York, 1955).

[29] In order to remove any ambiguity about the meaning of force constants we shall encounter later, we present, in the usual notation, the explicit form of several representative symmetry coordinates, or

$$S_{3a}=2^{-1/2}(\Delta r_5-\Delta r_6),$$

$$S_{4a}=8^{-1/2}r_e(\Delta\alpha_{15}+\Delta\alpha_{25}+\Delta\alpha_{35}+\Delta\alpha_{45}-\Delta\alpha_{16}-\Delta\alpha_{26}-\Delta\alpha_{36}-\Delta\alpha_{46}),$$

$$S_{5a}=(\tfrac{1}{2}r_e)(-\Delta\alpha_{12}+\Delta\alpha_{23}-\Delta\alpha_{34}+\Delta\alpha_{14}).$$

Except for the numbering scheme these coordinates are those of C. W. F. T. Pistorius, J. Chem. Phys. **29**, 1328 (1959). For identification of subscripts see Figs. 1 and 2.

[30] Y. Morino, S. J. Cyvin, K. Kuchitsu, and T. Iijima, J. Chem. Phys. **36**, 1109 (1962).

of amplitudes among the various modes will give rise to symmetrical radial distribution peaks. We conclude, therefore, that the pronounced asymmetry of the 2.7-Å F–F peak in the experimental radial distribution function *cannot possibly be due simply to large amplitudes associated with one or more independent normal modes of vibration of an octahedral molecule.* Either the molecule must be more or less frozen in a deformed configuration of the sort discussed in Sec. II, or else a breakdown of the simple normal-coordinate picture has occurred.

What is required to fit the diffraction data, mainly, is some sort of correlation in phase between t_{1u} and t_{2g} displacements. This, as we shall see, can skew the F–F distribution in the required manner. There are two natural mechanisms which can give rise to such correlation: Case (1) Jahn–Teller effect where *linear* potential-energy terms in the t_{2g} displacements lead to a spontaneous deformation (e.g., to Goodman's D_{3d} equilibrium configuration[10]). A mode corresponding to a t_{1u} bend and possessing a low force constant and suitable direction (e.g., the a_{2u} mode for Goodman's D_{3d} configuration) then executes large amplitudes of vibration about the deformed equilibrium configuration. Case (2), where the linear potential-energy terms are all zero but where t_{1u} bending modes have such large amplitudes of vibration that cubic and higher terms coupling the t_{1u} and t_{2g} modes have a strong influence on the molecular motion.

Case (1), the Jahn–Teller case, can be accommodated in the framework of the structural analyses of Sec. II which treat "statically deformed" structures, even if the interconversion between the several equivalent distorted forms is quite rapid.

A proper understanding of Case (2) requires a detailed consideration of the intramolecular motions involved. Since, in several ways, Case (2) presents a smaller departure from various lines of chemical intuition than Case (1), it seems warranted to explore it at some length. This is done in the next few sections.

Before leaving this section the question of uniqueness must be answered. Are there any other correlations of modes which will reproduce the observed skew in the F–F distribution? From Sec. II on static fits a resolution of the acceptable deformations into symmetry-coordinate components suggests that t_{1u} and t_{2g} are the principal contributors. The intuitive expectation that if $(t_{1u}+t_{2g})$ works, $(t_{1u}+e_g)$ might also, is fullfilled, qualitatively. Since e_g is a stretching coordinate, however, it turns out that sufficient e_g to skew the F–F peak splits the Xe–F peak an order of magnitude too much. For the same reason that e_g is less important than t_{2g}, the t_{1u} stretch is less important than the t_{1u} bend. Other combinations of symmetry coordinates are also found to be of minor utility.

D. Discussion of Soft t_{1u} Bending Mode

It has already been deduced from the electron-diffraction data that the fluorines in XeF_6 tend to avoid one region of the coordination sphere and compress together toward the opposite side. Of the coordinates in Fig. 3, it is apparent that the t_{1u} bending coordinates $S_{4a,b,c}$ and their linear combinations are the symmetry coordinates which best express such a displacement. The normal coordinates $Q_{4a,b,c}$ corresponding most closely to $S_{4a,b,c}$ no doubt contain a certain proportion of $S_{3a,b,c}$. Gillespie's picture[6,7] suggests that the stretching and bending coordinates as depicted in Fig. 3 combine to give normal coordinates Q_{4i} proportional to $(S_{4i}+\gamma S_{3i})$ etc., with $\gamma>0$. That is, the repulsive aspect of the lone pair tends to make the bonds which are closest to the lone pair the longest bonds. It turns out that most of what we conclude is insensitive to the proportion of $S_{3a,b,c}$ in $Q_{4a,b,c}$ and henceforth we shall discuss the $Q_{4a,b,c}$ as if they were essentially identical in form with $S_{4a,b,c}$. The other normal modes, namely Q_1, $Q_{2a,b}$, $Q_{5a,b,c}$, and $Q_{6a,b,c}$, *are* identical in form with the corresponding symmetry coordinates since they are grouped into orthogonal sets of species of different symmetries. In any event, the coordinates $Q_{4a,b,c}$ are prominently involved in the unusual properties of XeF_6. Since they correspond to an abnormally low force constant whether we accept the permanently deformed model (cf. Goodman's Jahn–Teller model)[10] or a dynamically inverting model, we shall refer to them as the "inversion" coordinates (although the t_{2g} coordinates might have a better claim to this designation if the Jahn–Teller model proves to be correct.)

Neglecting the possibility of a Jahn–Teller deformation, we can now rephrase the question "is XeF_6 a regular octahedron or is it distorted in its equilibrium structure?," alternatively as "is the force constant λ_4 for $Q_{4a,b,c}$ positive or negative?" It is helpful in visualizing the alternatives to recall that BH_3 and NH_3 may be treated as molecules with D_{3h} reference structures (planar equilateral triangles). The force constant for the out-of-plane bending displacement Q_2 of monomeric BH_3 is undoubtedly positive, leading to a D_{3h} equilibrium structure. On the other hand, the "Gillespie lone pair" which distinguishes NH_3 from BH_3 gives NH_3 a *negative* out-of-plane bending constant, causing the molecule to deform from D_{3h} symmetry spontaneously. In this representation it is the terms in $V(Q_i)$ which are quartic (and higher) in the inversion coordinate Q_2 that reverse the downward sweep of $V(Q_2)$ and establish the double minimum in the potential function.

It is entirely natural, then, to inquire for XeF_6 whether xenon's "lone pair" makes the t_{1u} force constant λ_4 *negative*, distorting the molecule. Higher-order terms, which we shall discuss in Sec. III.G, presumably prevent a excessive deformation. Whether the available evidence actually favors a negative value for λ_4 instead of merely a low value will be weighed in a following section. Although the analogy between the inversion of XeF_6 and the inversion of NH_3 is stressed in the foregoing picture, there is one profound difference between the cases. For NH_3 to invert it

must surmount or tunnel through the inversion barrier along the one-dimensional path available (Q_2). For XeF_6, however, the three-dimensional nature of the triply degenerate inversion mode provides a passageway for inversion in which a barrier at $Q_{4i}=0$ may be circumvented without cost of potential energy (to the quadratic approximation). In order to make this and other properties readily understandable, we shall examine the characteristics of the t_{1u} inversion mode.

Since the inversion coordinates Q_{4a}, Q_{4b}, and Q_{4c}, being equivalent except for direction, correspond to a degenerate set of normal modes, any linear combination of them is an equally acceptable normal coordinate. A particularly convenient method for identifying various linear combinations is to introduce a radial vector $\mathfrak{R}$ with directions θ and ϕ defined in terms of components

$$Q_{4a}=\mathfrak{R}\cos\theta, \tag{1a}$$

$$Q_{4b}=\mathfrak{R}\sin\theta\cos\phi, \tag{1b}$$

$$Q_{4c}=\mathfrak{R}\sin\theta\sin\phi. \tag{1c}$$

An inspection of the diagrams in Figs. 2 and 3 will reveal at once that the direction of $\mathfrak{R}$ is the direction of the "Gillespie lone pair," and the magnitude of $\mathfrak{R}$ establishes the degree of deformation from O_h symmetry. Referring to Fig. 2, we note that if $\mathfrak{R}$ is directed toward a corner, face center, or edge center of the octahedron, a C_{4v}, C_{3v}, or C_{2v} configuration will result.

An especially helpful way to visualize the infinite variety of t_{1u} deformations encountered in the three-dimensional inversion problem is to consider the model illustrated in Fig. 4. The three inversion coordinates Q_{4a}, Q_{4b}, and Q_{4c} are related to the three Cartesian coordinates of Point i in the figure. The coupling of the stretch $S_{3a,b,c}$ and bend $S_{4a,b,c}$ motions in the actual displacements of ligands in the model is illustrative of the coupling which doubtless occurs in $Q_{4a,b,c}$ but the magnitude of the coupling in the model is purely schematic (it can be controlled by the size of the central xenon sphere).

Expressed in terms of the spherical polar coordinates $\mathfrak{R}$, θ, and ϕ, the potential energy for inversion becomes, through quadratic terms

$$2V_4(\mathfrak{R})=\lambda_4(Q_{4a}^2+Q_{4b}^2+Q_{4c}^2)$$
$$=\lambda_4\mathfrak{R}^2, \tag{2}$$

in which the dependency on ϕ and θ drops out. An inversion of the molecule from a configuration $\mathfrak{R}_m$ to a configuration $\mathfrak{R}_n$, then, requires no change in potential energy if $\mathfrak{R}$ is constant, according to Eq. (8), even if a *linear* path connecting the configurations goes through a large potential-energy barrier. If λ_4 is negative, the simplest correction to give $V_4(\mathfrak{R})$ an acceptable form is

$$2V_4(\mathfrak{R})=-|\lambda_4|\mathfrak{R}^2+k_{4444}\mathfrak{R}^4, \tag{3}$$

although there is nothing about the symmetry of the problem which demands that terms higher than quadratic be independent of θ and ϕ. Indeed, there is compelling evidence that changing the direction of $\mathfrak{R}$ actually does change the potential energy of the molecule significantly. This is discussed in the following sections.

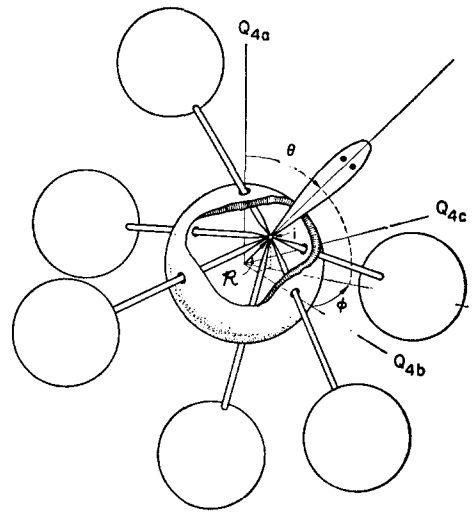

FIG. 4. Model illustrating the relationship between atomic positions, the normal coordinates Q_{4a}, Q_{4b}, and Q_{4c}, and the t_{1u} polar coordinates $\mathfrak{R}$, θ, and ϕ. The coupling of atomic motions in the ν_4 mode corresponds the joining of the bond termini inside the central atom by a flexible link at point i. The vector $\mathfrak{R}$, with components Q_{4a}, Q_{4b}, and Q_{4c}, radiates from the origin to point i and lies along the lone-pair axis. As the lone pair sweeps around the central atom, the ligands avoid it, and bonds close to the lone pair become longer than those more remote.

E. Coupling of Other Modes With t_{1u} Mode

As pointed out in Sec. III.C, the alternative to accepting a statically deformed structure for XeF_6 is to assume that a breakdown of normal-coordinate theory has occurred. Now, a breakdown of a theory derived on the basis of infinitesimal vibrations would hardly be surprising in the case of XeF_6. Potential-energy functions of real molecules contain higher-order terms connecting the coordinates of different symmetries, and these terms cannot be neglected if displacements are large. In ammonia and other inverting NX_3 molecules the breakdown is only modest since, to within well-understood limits of approximation, the molecules can be considered to be executing vibrations of small displacement in one of the two basins of $V(Q_1, Q_2, Q_3)$. In XeF_6 the breakdown is more conspicuous because the molecule is much more crowded than NH_3 and, unlike NH_3, has ligands which become nonequivalent at various intervals during the inversion process. Steric (and perhaps, other) stresses in XeF_6 are exerted differently upon different ligands, causing a distortion from pure t_{1u} symmetry in the inversion mode which has no counterpart in NH_3. It is this distortion, or what is the same thing, this induced correlation between the coordinates of different symmetry, which offers us what is perhaps the simplest interpretation of the observed electron-diffraction data.

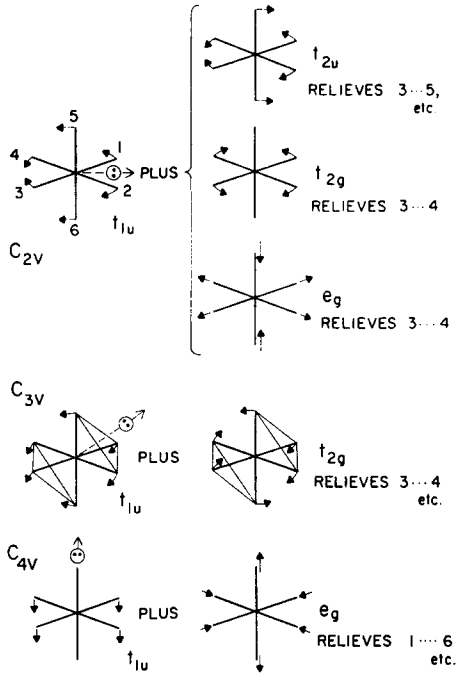

FIG. 5. Diagrams indicating how the steric strain incurred in t_{1u} deformations to C_{2v}, C_{3v}, and C_{4v} can be relieved by a mixture of different symmetry species.

To see what form this mixing of different symmetries may assume, it is helpful to examine the diagrams in Fig. 5. By inspection it can be seen which modes will mix with t_{1u} at various symmetries if the interactions are steric. Note that C_{2v}, C_{3v}, and C_{4v} t_{1u} displacements correspond to the mixtures $S_{4b}+S_{4c}$, $S_{4a}+S_{4b}+S_{4c}$, and S_{4a}, respectively, or equivalent combinations. Formal considerations of cubic and quartic potential-energy terms show that the mixing implied by Fig. 5 is not limited to purely steric interactions. Since the onset of the symmetry-breaking interactions illustrated occurs at more or less definite phases of the inversion mode, it is evident that the various admixed modes in the inversion will be correlated in phase with the t_{1u} displacements. The effect of this on the electron-diffraction intensities and on spectroscopic selection rules will be discussed in the following sections.

F. Simplified Model of Correlated Modes

The aim of this section is to demonstrate that the principal characteristics of the experimental radial distribution function $f(r)$ in the 2.7-Å region can indeed be reproduced by a model of correlated normal coordinates. To relate the $f(r)$ distribution to the symmetry coordinates we expand a representative nonbonded distance F_1–F_2 in terms of the symmetry coordinates. Through linear terms the result is

$$r_{12}=2^{1/2}r_{\mathrm{XeF}}+3^{-1/2}S_1-6^{-1/2}S_{2a}-8^{-1/2}S_{5a}$$
$$+0.25[2(S_{3b}+S_{3c})+(S_{4b}+S_{4c})+(S_{6b}-S_{6c})]. \quad (4)$$

The primary effect of vibrations Q_1, Q_{2a}, Q_{5a}, and $Q_{6b,c}$ is to broaden the distribution $f(r_{12})$ somewhat. We assume, for simplicity, that Q_{3b} and Q_{3c} also only broaden the distribution without contributing to its unusual shape. We neglect the difference in form between normal and symmetry coordinates. For the inversion mode we neglect the admixing of the e_g and t_{2u} coordinates and consider only the most important impurity coordinates, the t_{2g} coordinates (of which only S_{5a} influences r_{12} in first order). In connecting S_{4b}, S_{4c}, and S_{5a} it is necessary to comply with the following requirements: (1) For infinitesimal inversion displacements the inversion cordinates should be of pure t_{1u} symmetry. (2) From Fig. 5 it is clear for a large displacement $(S_{4b}+S_{4c})$ to C_{2v} symmetry that S_{5a} must be taken as negative whether $(S_{4b}+S_{4c})$ is negative or positive. (3) Similarly, for a large displacement $(S_{4b}-S_{4c})$ which is orthogonal to $(S_{4b}+S_{4c})$, S_{5a} must be taken as positive irrespective of the sign of $(S_{4b}-S_{4c})$. (4) For any C_{4v} displacement such as S_{4b} or S_{4c}, S_{5a} must be zero. The simplest functional relationship obeying these conditions is

$$S_{5a}=C'[(S_{4b}+S_{4c})^2-(S_{4b}-S_{4c})^2] \quad (5)$$
$$=4C'S_{4b}S_{4c}.$$

Our treatment of the effect of the inversion on r_{12} then reduces, upon simplifying Eq. (4) by inclusion of only t_{1u} and t_{2g} coordinates and introducing Eq. (5), to

$$r_{12}=2^{1/2}r_{\mathrm{XeF}}+0.25[(S_{4b}+S_{4c})+CS_{4b}S_{4c}], \quad (6)$$

where C is a freely adjustable constant. Such a rigid correlation between the t_{2g} and t_{1u} coordinates in the inversion mode is obviously an oversimplification. It is a useful oversimplification in illustrating the consequences of correlation between coordinates, however, and the essential validity of its general form is rationalized in the following sections.

Let us introduce the spherical polar coordinates R, θ, and ϕ analogous to those of Eq. (1) to represent S_{4a}, S_{4b}, and S_{4c}. The nonbonded distribution function $P(r_{12})$ for distance r_{12} can be generated by sweeping the inversion vector $\mathbf{R}$ over its distribution function $\rho(\mathbf{R})$. Since all fluorines are equivalent in the space average distribution, the distribution $P(r_{12})$ is representative of the distribution for all adjacent pairs of fluorines in XeF_6. In order to compare the calculated distribution with experiment it is necessary to include the broadening due to the other vibrational modes and to convert $P(r)$ to the conventional electron-diffraction distribution $f(r)$. This was done as follows. For each value of $r_{12}=r_{12}(R_i, \theta_j, \phi_k)$ a component $f(r)$ curve was calculated according to

$$f(r)_{ijk}=\frac{C_{12}}{r_{12}}\left\{\frac{a}{\gamma}\exp\left[\frac{-(r-r_{ijk})^2}{2\gamma^2}\right]+\frac{b}{\delta}\exp\left[\frac{-(r-r_{ijk})^2}{2\delta^2}\right]\right\} \quad (7)$$

where, in the notation of Paper I,[8] $\gamma^2=2b_0+l^2$ and $\delta^2=2b_0+2\beta+l^2$ include the Degard factor b_0, the planetary electron parameters a, b, and β, and the skeletal

amplitude of vibration l. The total $f(r)$ function is a sum of all components weighted by the distribution $\rho(R_i, \theta_j, \phi_k)$, or

$$f(r) = \sum \sum \sum w_{ijk} f(r)_{ijk}. \quad (8)$$

The skeletal amplitude l was taken as 0.06 Å, its approximate value in other hexafluorides, but results are insensitive to the exact value.

Results of numerical calculations of $f(r)$ for a variety of different distributions assumed for $\rho(R)$ are shown in Fig. 6. It is apparent at a glance that the skew of the experimental curve is reproduced approximately if, *and only if*, the t_{2g} "impurity coordinate" is of substantial amplitude and is correlated in phase with the inversion coordinate. That is, only if the mixing coefficient C of Eq. (6) is rather large is the calculated 2.7-Å $f(r)$ peak similar to the experimental peak.

The $\rho(R)$ distribution anticipated for an O_h equilibrium structure perturbed by potential terms higher than quadratic would have an approximately Gaussian radial dependence and a more or less spherically symmetric distribution in θ and ϕ, provided that the higher-order terms were small compared with kT. Of the spherically symmetric $\rho(R)$ functions tested, including Gaussian, square (particle in spherical box), and broadened "spherical shell" functions, none is markedly better than the other provided the scale factor is adjusted to make the mean value $\langle R \rangle$ about 0.9 Å. Still better fits might be obtainable with a spherically symmetric $\rho(R)$ if t_{2u} and e_g coordinates were mixed in with the t_{2g} and t_{1u}. Such a complicated model has not been explored.

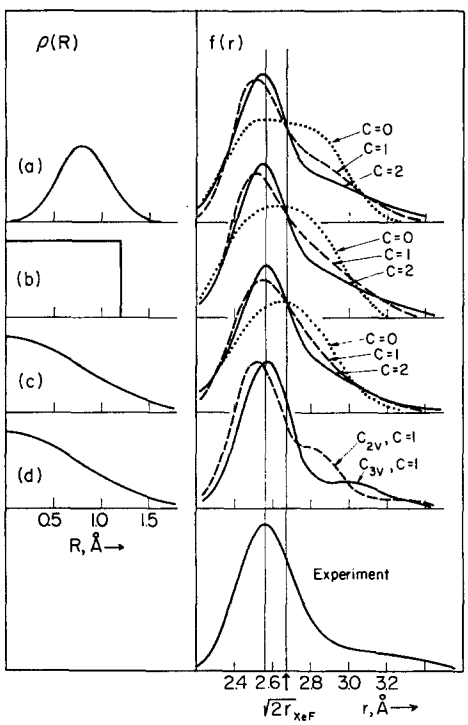

FIG. 6. Geminal F–F radial distribution functions $f(r)$ calculated by simplified model of correlated modes (Sec. III. F), for various postulated t_{1u}, t_{2g} distributions $\rho(R)$. The distributions (a)–(c) correspond to spherically symmetric $\rho(R)$ functions. The distribution (d) corresponds to a Gaussian function in R but completely localized C_{2v} or C_{3v} functions in θ and ϕ. A radial shrinking of $\rho(R)$ has the effect of shrinking the $f(r)$ function to a narrower peak with a center of gravity at 2.67 Å. The slight skew for $C=0$ results from the fact that $f(r)$ is defined in terms of $r^{-1}P(r)$ rather than $P(r)$ itself.

TABLE III. Symmetry-allowed cubic terms $V(Q_i, Q_j, Q_k)$ in the potential-energy function of an XY_6 molecule.

i,j,k	i,j,k	i,j,k	i,j,k	i,j,k
111	155	233	266	345
122	166	244	236	356
133	134	234	246	445
144	222	255	335	456
				566

Spherically symmetric distributions in R, of course, correspond to cases where the "lone pair" has the same probability of protruding in any one direction as in any other. Although this distribution would be required for a purely quadratic potential function, it is inconsistent with a significant contribution from the cubic terms coupling the t_{1u} and t_{2g} modes. These terms introduce a bias away from C_{4v} structures of just the sort which would be expected according to the spirit of the valence shell electron-pair repulsion model. The best $\rho(\mathbf{R})$ functions are in accord with a t_{1u}, t_{2g} perturbation and with the electron-pair repulsion model; they favor distributions in which the lone-pair vector $\mathbf{R}$ avoids the bonding pairs.

Two interesting factors complicate the drawing of an unequivocal decision about the distribution function $\rho(\mathbf{R})$ from the experimental $f(r)$ curve. The first stems from the novel three-dimensional nature of the inversion. Just as the 1s orbital of a hydrogen atom has the greatest probability density, $\rho(r)$ at $r=0$ while having the most probable value of r at the Bohr radius a_0, it is possible for XeF_6 that $\rho(R)$ is greatest at $R=0$ (i.e., at the O_h configuration) even though the most probable R value corresponds to an appreciably distorted configuration. The R^2 weighting of the radial distribution curve $4\pi R^2\rho(R)$ makes the diffraction data insensitive to the density function at small R. The second complication is that even a spherically symmetrical distribution gives the $f(r)$ curve a bias toward the C_{2v} configuration. As the inversion mode vector $\mathbf{R}$ sweeps around the coordination sphere it generates 12 different C_{2v} structures, eight C_{3v} structures, and only six C_{4v} structures since an octahedron has 12 edges, eight faces and six vertices.

G. Higher-Order Terms in XeF_6 Potential Function

The symmetry-allowed cubic terms are indicated in Table III. Orders of magnitude of many of the cubic constants can be derived from model force fields as described previously.[31] Cubic terms involving the

[31] K. Kuchitsu and L. S. Bartell, J. Chem. Phys. **36**, 2460, 2470 (1962).

a_{1g} coordinate are undoubtedly important in determining the mean bond lengths but they do not influence the shape of the molecule. In the following we shall examine only those terms which seem of consequence in accounting for the unusual features of the electron-diffraction results. These are the terms that lower the potential energy when coordinates mix in the sense indicated schematically in Fig. 5.

A representative term lowering $V(Q_i)$ for large $(Q_{4b}+Q_{4c})$ when Q_{5a} is negative, irrespective of the sign of $(Q_{4b}+Q_{4c})$, is

$$k_{445}'(Q_{4b}+Q_{4c})^2Q_{5a}.$$

If we use the O_h symmetry operations to generate the sum of such terms consistent with the over-all symmetry required, we find

$$V_{445}=k_{445}(Q_{4b}Q_{4c}Q_{5a}+Q_{4a}Q_{4c}Q_{5b}+Q_{4a}Q_{4b}Q_{5c}), \quad (9)$$

in which we expect k_{445} to be positive to express the stress incurred when the backside equatorial atoms or bonds bump each other. The corresponding quartic terms preventing an excessive overcorrection at large Q_5 are

$$V_{4455}=k_{4455}[(Q_{4b}^2+Q_{4c}^2)Q_{5a}^2+(Q_{4a}^2+Q_{4c}^2)Q_{5b}^2+(Q_{4a}^2+Q_{4b}^2)Q_{4c}^2], \quad (10)$$

with $k_{4455}>0$. The term V_{4444} discussed below also can compensate for the behavior of V_{445} at large deformations. A sufficiently large value of k_{445} can lead to a potential-energy minimum away from O_h symmetry even if all quadratic constants are positive

The leading terms expressing the tendency of axial bonds to avoid equatorial bonds in C_{2v} configurations interrelate t_{2u} and t_{1u} according to

$$V_{4446}=k_{4446}[(Q_{4b}+Q_{4c})^3(Q_{6b}-Q_{6c})+(Q_{4b}-Q_{4c})^3(Q_{6b}+Q_{6c})+(Q_{4a}+Q_{4b})^3(Q_{6a}-Q_{6b})+(Q_{4a}-Q_{4b})^3(Q_{6a}+Q_{6b})-(Q_{4a}+Q_{4c})^3(Q_{6a}-Q_{6c})-(Q_{4a}-Q_{4c})^3(Q_{6a}+Q_{6c})], \quad (11)$$

in which k_{4446} is presumably *negative*. No cubic terms expressing this bond–bond avoidance arise.

An admixture of e_g coordinates with t_{1u} coordinates in the inversion is effected by the cubic terms

$$V_{442}=k_{442}[2Q_{4a}^2Q_{2a}+Q_{4b}^2(3^{1/2}Q_{3b}-Q_{2a})-Q_{4c}^2(3^{1/2}Q_{2b}+Q_{2a})], \quad (12)$$

in which steric interactions tend to make k_{442} negative. Corresponding quartic terms to compensate at large negative Q_2 values are of the form

$$V_{4422}=k_{4422}[4Q_{4a}^2Q_{2a}^2+Q_{4b}^2(3^{1/2}Q_{2b}-Q_{2a})^2+Q_{4c}^2(3^{1/2}Q_{2b}+Q_{2a})^2]. \quad (13)$$

If the higher-order cross terms between t_{1u} and other coordinates are significant we must surely expect the higher-order terms of t_{1u} itself to be significant. Symmetry rules out cubic terms. Besides the spherically symmetric quartic term of Eq. (3) we must expect a term

$$V_{4444}=k_{4444}'(Q_{4a}^3+Q_{4b}^4+Q_{4c}^4), \quad (14)$$

in which the sign of k_{4444}' is negative for a purely steric perturbation.

The higher-order contributions of Eqs. (9)–(14) are the most obvious terms capable of causing the observed correlations between the various vibrational modes. These perturbing terms remove the iostropy of $V(Q_i)$ with respect to the t_{1u} "lone-pair" vector **R**. The t_{2g} term V_{445} stabilizes the C_{2v} and C_{3v} configurations, but not the C_{4v} configuration. The e_g term V_{442} stabilizes C_{2v} and C_{4v} but not C_{3v}.

It is pertinent to say a few words about an aspect which may seem puzzling at first glance. The theme of our discussion of the higher-order terms has so far been that they may arise from steric or quasisteric interactions. Neverthless, the leading interactions V_{445}, V_{442}, and V_{4446} become negative for certain molecular configurations and hence are stabilizing for these configurations relative to the purely quadratic force field. How is it that purely repulsive interactions can lead to a stabilizing, *lowering* of potential energy? The answer, of course, is that purely repulsive interactions cannot lower the potential-energy relative to the potential energy in the absence of the repulsive interactions. The point is that the repulsive interactions have components in the quadratic as well as in the higher terms. In the absence of repulsive interactions the quadratic force constants would be lower, and the quadratic force field would be everywhere lower than the net (quadratic plus higher degree) field in the presence of repulsive interactions.

H. Connection between the Constants of Secs. III. F and III. G

Though cubic terms, the potential energy of XeF_6 depends upon the t_{1u} bend and t_{2g} coordinates according to

$$2V(S_4, S_5)=F_{44}(S_{4a}^2+S_{4b}^2+S_{4c}^2)+F_{55}(S_{5a}^2+S_{5b}^2+S_{5c}^2)+2F_{445}(S_{4a}S_{4b}S_{5c}+S_{4b}S_{4c}S_{5a}+S_{4c}S_{4a}S_{5b}). \quad (15)$$

For any given values of the t_{1u} coordinates it is easily seen that $V(S_4, S_{5a})$ has a minimum value for

$$S_{5a}(\min)=-(F_{445}/F_{55})S_{4b}S_{4c}. \quad (16)$$

Clearly, then, S_{5a} tends to be related to the t_{1u} coordinates in just the manner implied by the simple model of Eq. (5), Sec. III.F, and we may associate the constant C of Eq. (6) with F_{445} and F_{55} by the approximation

$$C\approx 2^{1/2}F_{445}/F_{55}. \quad (17)$$

From the curve fits associated with Fig. 6, it is possible to deduce an order of magnitude for C, and hence, for

F_{445}, if F_{55} is known. This provides some insight into the nature of the interactions responsible for coupling the modes.

To identify the cubic constant F_{445} with that of a steric model we note that the 2.7-Å nonbonded components of the potential function can be expanded as

$$V_{\rm nb}=\sum\left[V_{ij}{}^0+\left(\frac{\partial V_{ij}}{\partial q_{ij}}\right)_0\Delta q_{ij}+\frac{1}{2}\left(\frac{\partial^2 V_{ij}}{\partial q^2{}_{ij}}\right)_0(\Delta q_{ij})^2+\frac{1}{6}\left(\frac{\partial^3 V_{ij}}{\partial q_{ij}{}^3}\right)_0(\Delta q_{ij})^3+\cdots\right], \quad (18)$$

where q represents a nonbonded distance and Δq is its displacement from the reference value. For t_{1u} bend and t_{2g} deformations, according to Eq. (4), we may take

$$\Delta q_{12}=0.25(S_{4b}+S_{4c})+8^{-1/2}S_{5a}+\cdots, \quad (19)$$

so that

$$\sum(\Delta q_{ij})^3=-(3/32^{1/2})\times(S_{5a}S_{4b}S_{4c}+S_{5b}S_{4c}S_{4a}+S_{5c}S_{4a}S_{4b})+\cdots. \quad (20)$$

Neglecting higher-order terms of Eq. (19), substituting Eq. (20) into Eq. (18), and comparing the result with Eq. (15) we identify the steric contribution $(F_{445})_{\rm nb}$ as

$$(F_{445})_{\rm nb}\approx-(2^{1/2}/16)(\partial^3 V_{ij}/\partial q_{ij}{}^3)_0. \quad (21)$$

If, further, we assume that

$$V_{\rm nb}(q_{ij})=Aq_{ij}{}^{-n}, \quad (22)$$

Eq. (21) can be expressed as

$$(F_{445})_{\gamma p}=[2(n+2)/32r_{\rm XeF}]F_{\rm FF}, \quad (23)$$

where $F_{\rm FF}$ is the Urey–Bradley constant $(\partial^2 V_{ij}/\partial q_{ij}{}^2)_0$, the approximate magnitude of which is known. Now, since the curve fittings of Sec. III.F suggest that the coupling constant C has a value of approximately 2 Å^{-1}, we infer from Eq. (17) that

$$F_{445}\approx 2^{-1/2}CF_{55}\approx 0.4\,\text{mdyn/Å}^2, \quad (24)$$

assuming that $F_{55}\approx 0.28$ mdyn/Å (as calculated from the assignment of the 317-cm^{-1} Raman band as ν_5).[32] To estimate the steric contribution, we take Eq. (23) with $n\approx 10$ and $F_{\rm FF}\approx 0.04$ mdyn/Å, the value appropriate for 2.7-Å interactions,[33] and obtain

$$(F_{445})_{\rm nb}\approx 0.02\ \text{mdyn/Å}^2. \quad (25)$$

This result is so much lower than the value estimated from the diffraction data that we conclude, tentatively, that the conspicuous coupling between the t_{1u} and t_{2g} modes is induced by interactions stronger than simple steric forces.

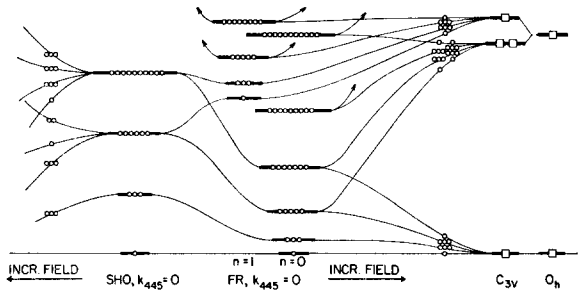

FIG. 7. Correlation diagram relating ν_4 vibrational levels for XeF_6 according to an O_h equilibrium (SHO) model with an extremely low force constant, a free rotator (FR) model with *negative* quadratic force constant F_{44}, a statically deformed C_{3v} model, and a normal O_h model. A particle-in-a-spherical-box model fitting the diffraction data [cf. Fig. 6(b)] would give levels intermediate between the SHO and FR levels. The splitting of levels to the left of the SHO model and to the right of the FR model can be envisioned as the octahedral "crystal-field" splitting by the t_{1u}, t_{2g} coupling potential.

IV. INFERENCES ABOUT t_{1u} FREQUENCY

Although information on the potential-energy function of XeF_6 is still very meager it is possible to make some inferences from the diffraction data about the inversion mode which may help in its spectroscopic identification. We shall discuss three limiting cases, namely (a) a harmonic oscillator (SHO) model with $F_{44}>0$, (b) a free-rotator (FR) model with $F_{44}<0$, and (c) a static deformation (SD) model. Intermediate situations and effects of perturbing fields are portrayed in the correlation diagram of Fig. 7. As before, it is to be understood that we are discussing the normal coordinates of the inversion mode but in our rough-and-ready calculations we shall not distinguish between the form of the bending t_{1u} normal coordinates and symmetry coordinates. The effective mass[28] associated with motion of the system in the coordinates S_{4a}, S_{4b}, and S_{4c} will be taken as the matrix element $(G^{-1})_{44}$ which has a value of 6.56 g/mole.

For the SHO model it is envisioned that the potential-energy function has a minimum at O_h symmetry. From the curve fitting associated with Fig. 6 we infer that the harmonic-oscillator thermal distribution,

$$\rho(R)=A\exp(-R^2/2l^2), \quad (26)$$

has a characteristic amplitude l of roughly 0.5_5 Å. Such a large amplitude of vibration implies a small force constant, so that the classical law of equipartition of energy should be satisfied, or

$$3kT=(F^{-1})_{44}{}^{-1}(\langle S_{4a}{}^2\rangle+\langle S_{4b}{}^2\rangle+\langle S_{4c}{}^2\rangle)\approx 3F_{44}l^2, \quad (27)$$

from which we can obtain the crude value for F_{44} of

[32] H. H. Claassen, Bull. Am. Phys. Soc. **12**, 295 (1967); (private communication).

[33] Value represents an extrapolation of $F(q_{\rm FF})$ values given by Shimanouchi *et al.* to the F–F distance in XeF_6 at O_h symmetry, [T. Shimanouchi, I. Nakagawa, J. Hiraishi, and M. Ishii, J. Mol. Spectry. **19**, 78 (1966)], and agree with $(\partial^2 V/\partial q^2)$ for Ne–Ne interactions at the same distance [J. O. Hirschfelder, C. F. Curtiss, and R. B. Bird, *Molecular Theory of Gases and Liquids* (John Wiley & Sons, Inc., New York, 1964)].

$\approx$0.01 mdyn/Å. Inserting this value into

$$\nu_4 \approx (2\pi)^{-1}[F_{44}/(G^{-1})_{44}]^{1/2},$$

we obtain a frequency of $\nu_4 \approx 60$ cm^{-1}.

The SHO model with an O_h equilibrium structure is only able to account for the diffraction data if a strong mixing with t_{2g} is invoked. This mixing is presumably due to the cubic terms of Eq. (9). A little reflection confirms that this perturbation, when averaged over the coordinates of $S_{5a,b,c}$ with the use of a properly correlated wavefunction, corresponds to a field which is octahedral in the t_{1u} space. That is, deformations to C_{3v} structures are less costly than deformations to C_{4v}. Since the vibrational wavefunctions of an isotropic three-dimensional SHO have the same angular dependency as atomic orbitals, the splitting of the ν_4 energy levels by an octahedral field is quite analogous to the well-known crystal-field splitting of atomic levels.[34] This splitting is shown to the left of the SHO levels in Fig. 7. The magnitude of F_{445} suggested in Sec. III.G indicates that the splitting is *large*. Because the effect of the cubic terms is to *lower* the potential energy for delocalization in C_{3v} directions, the root-mean-square amplitude l derived above is probably *larger* than the amplitude for the quadratic problem.

For the free-rotator model it is assumed that the potential-energy function $V(R, \theta, \phi)$ for inversion has the form

$$2V(R, \theta, \phi) = F_{44}R^2 + F_{4444}R^4 \qquad (28)$$

and that F_{44} is large and negative. The quartic term is considered to be adjusted to put the potential minimum at the value R_e associated with curve fit of Fig. 6. In this model, in contrast to the SHO model, there is a barrier to inversion via a path through the O_h configuration. One virtue of the FR model is that the result we seek is essentially independent of the barrier as long as the barrier is reasonably high. That is, if the potential well is deep enough at $R = R_e$, the potential energy of Eq. (28) corresponds exactly to that of a rotating diatomic molecule [except that the skew of $V(R-R_e)$ from quadratic is opposite in sign to that of a Morse oscillator]. Therefore, to this approximation, the t_{1u} inversion energy levels can be represented by the diatomic molecule expression,

$$E_{n,T}(\text{inv}) = E_n(\text{vib}) + E_T(\text{rot}). \qquad (29)$$

The "rotational" inversion frequencies will be so much lower than the "vibrational" inversion frequencies that we can treat the separation of the inversion multiplets in terms of the "rotational" inversion energies

$$E_T = J(J+1)^{+2}/2\mathrm{I}_{\text{inv}}. \qquad (30)$$

The effective moment of inertia for the inversion is

$$\mathrm{I}_{\text{inv}} = (G^{-1})_{44}R_0^2. \qquad (31)$$

For a broadened "spherical shell" $\rho(R)$ model, the value of R giving a fit with the diffraction data is $\langle R \rangle \approx 0.9$ Å. For Fig. 6(a), this corresponds to an $\langle R^{-2} \rangle^{-1/2}$ value of $R_0 \approx 0.7_5$ Å and a value of I_{inv} which is 74 times smaller than the moment of inertia for true rotation of XeF_6. According to this model, then, the inversion frequencies are 74 times higher than the corresponding rotational frequencies with the lowest ($J=0$ to $J=1$) transition occurring at roughly 10 cm^{-1}.

The static deformation model is derived from the free-rotator model by adding an angular dependency to $V(R, \theta, \phi)$ in order to stabilize strongly a configuration at $V(R_e, \theta_e, \phi_e)$. The minima of $V(R, \theta, \phi)$ are again presumably at C_{3v} configurations, just as they were for the SHO model. In the limit of deep potential minima at R_e, θ_e, ϕ_e (and at corresponding points generated by the O_h symmetry operations) the XeF_6 molecule would simply become a statically deformed molecule. The case intermediate between the free-rotator model and static deformation model is more interesting. It corresponds to an inversion problem analogous to that of NH_3 but more complex. While NH_3 has two minima in one dimension (Q_2), a C_{3v} stabilized XeF_6 has *eight* minima in *three* dimensions (Q_{4a}, Q_{4b}, Q_{4c}). The solutions of the more complex problem near the free-rotator limit again correspond to those of the crystal-field model, as illustrated in the correlation diagram of Fig. 7. To the right of the free-rotator limit the s-like, p-like, d-like, etc., inversion states are split by the octahedral field in the familiar way. Further to the right, the levels regroup and clusters of eight states are found. These inversion octuplets are easily seen to arise from the vibrational solutions derived from a trial wavefunction which is constructed from a linear combination of the appropriate eight localized t_{1u} vibrational wavefunctions corresponding to the eight C_{3v} potential minima. As a progressively stronger field freezes the molecule into a static deformation the multiplets collapse to the levels expected for a C_{3v} structure. The splitting of the levels would seem to be a rather large fraction of the zeroth-order energy of the level according to the magnitude of F_{445} suggested in Sec. III.G.

V. INTERACTIONS WITH ELECTROMAGNETIC FIELDS

Of the models proposed in the previous section, only the static deformation model would predict a pure rotational absorption spectrum for XeF_6. If the inversion splitting exceeded the rotational frequencies, however, in a model intermediate between the SD and FR limits, the spectral appearance would change markedly. The lowest dipole allowed transitions would be inversion lines with rotational structure instead of rotational lines split by inversion multiplets. The negative result of a preliminary search for the microwave spectrum of XeF_6 by Wilson *et al.*[35] suggests but

[34] T. M. Dunn, D. S. McClure, and R. G. Pearson, *Crystal Field Theory* (Harper and Row Publishers, Inc., New, York, 1965).

[35] E. B. Wilson, Jr. (private communication).

does not prove that XeF_6 is significantly to the left of the C_{3v} SD model of Fig. 7.

In our preliminary interpretations based on the rather poor scattering factors of Analysis I,[9] and on a much cruder computation of synthetic radial distribution curves, a perturbed FR model looked more promising than a perturbed SHO model. This, coupled with the implication by the Gillespie and the MO models that $F_{44}<0$, induced one of us (L.S.B.) to speculate on some spectroscopic properties of the FR model.[36] The preliminary estimate of $R_0=1$ Å corresponded to a $J=0$ to $J=1$ inversion transition of about 6 cm^{-1} and led Kim, Claassen, and Pearson[37] to search the submillimeter microwave spectrum from 3 to 8 cm^{-1}. No transitions were detected.

Of special interest is the appreciable t_{2g} component in the nomially t_{1u} inversion mode. This component should make the inversion mode strongly Raman active as well as far-infrared active even in the SHO and FR models. Since the t_{2g} vibrational phase is positive both for positive and negative t_{1u} phases, the t_{2g} impurity frequency for the SHO model is twice ν_4 and the SHO Raman selection rule should be $\Delta v=\pm 2$. The corresponding selection rule for the FR model is the rigid-rotator selection rule of $\Delta J=\pm 2$. Even in the absence of strong t_{2g} mixing the above Raman transitions are symmetry allowed. Ordinarily such overtone transitions are very weak, however.[38] Combination bands involving the closely spaced t_{1u} levels and hot bands associated with the large number of low-lying excited vibrational states should lead to a spectrum which is diffuse and difficult to interpret. Such seems to be the case.[3,26,39]

The diffraction data are not incompatible with an O_h equilibrium structure of XeF_6 (perturbed SHO model). It is well to point out that the selection rules for this case *and* the FR case (which does *not* have an O_h equilibrium structure) are formally those for O_h symmetry in the same sense as the selection rules for NH_3 are those for D_{3h} symmetry. If, however, the resolving power is insufficient to resolve the combination bands involving separate inversion levels (or low-frequency t_{1u} levels, as the case may be) the spectral characteristics will appear to be those for a nominally C_{3v} molecule, both for XeF_6 and NH_3.

The observation that fluorines are all equivalent in the long time scale of NMR spectra[40] is consistent with all models proposed in this section except the static deformation model in its extreme limit. Nuclear quadrupole resonance results might be helpful if it were possible to study the inversion frequencies under high enough resolution in the vapor phase. The static deformation and free-rotator models predict xenon nuclear quadrupole splitting, but, contrary to first impressions, the perturbed O_h harmonic-oscillator model with vibrations of large amplitude in well-defined states, also predicts splittings.

The absence of a measurable dipole moment in a molecular-beam experiment by Falconer, Büchler, Stauffer, and Klemperer[25] deserves comment. This experiment in which a molecular beam was subjected to an inhomogeneous electrostatic field, unequivocally demonstrates that XeF_6 is not a *rigid, polar* molecule. If the molecule is inverting, the sensitivity of the experiment decreases as the inversion frequency increases. Falconer *et al.* estimated how this sensitivity depends on the inversion splitting. According to this analysis, the maximum value of a dipole moment which is consistent with the beam experiment is given in debyes, for a one-dimensional double minimum model, by

$$\mu<0.1(\Delta E)^{1/2}, \tag{32}$$

where ΔE is the separation, in cm^{-1}, between inversion doublets. The sensitivity for the three-dimensional FR model is several-fold lower. For the present free-rotator model of inversion, then a dipole moment of nearly 1 D is not ruled out. Inasmuch as $XeOF_4$, which is more "distorted" than XeF_6, has a dipole moment of about 0.65 D,[41] the molecular-beam result does not provide a very delicate criterion for choosing between models. It only eliminates the asymmetric static deformations.

It is perhaps worth noting that if a model of fixed bond dipole moment is adopted for XeF_6, the best single configuration C_{2v} model of Sec. II has a molecular moment about half as large as an Xe–F bond moment. The C_{3v} model implies a molecular moment of only about 0.2 of a bond moment. Even these numbers overemphasize the electric moments. Molecular-orbital calculations show that the charges on fluorines redistribute as the molecule undergoes an ungerade deformation from O_h to a polar structure. This redistribution is of a direction and magnitude to cancel in fair measure the resultant molecular dipole moment. Ligands adjacent to the "lone-pair site" are the more negative, then, and the polarity of the deformed molecules must be quite low. An exactly analogous situation apparently occurs in XeF_4 where the ir-active e_u bending mode, believed by Claassen to be at about 170 cm^{-1}, has such a feeble transition moment as to elude detection in the gas phase.[39]

VI. RELATION TO VALENCE THEORY

Several review articles[1–3,42] on noble-gas compounds have discussed the bonding in XeF_6. The problem is too complex for a definitive, *a priori* treatment of the equilibrium geometry of the molecule by current theoretical methods. In the light of our present struc-

[36] L. S. Bartell, J. Chem. Phys. **46**, 4530 (1967).
[37] H. Kim, H. H. Claassen, and E. Pearson (private communication).
[38] G. Herzberg, *Infrared and Raman Spectra of Polyatomic Molecules* (D. Van Nostrand Co., Inc., Princeton, N.J., 1945), p. 264.
[39] H. H. Claassen (private communication).
[40] J. C. Hindman and A. Svirmicks, Ref. 1, p. 251.
[41] J. Martins and E. B. Wilson, Jr., as quoted in Ref. 25.
[42] D. S. Urch, J. Chem. Soc. **1964**, 1442.

tural study, however, we shall examine the consequences of several simple theoretical models which predict or rationalize a nonoctahedral symmetry for XeF_6. No attempt will be made to review the problem exhaustively or with rigor. The models will include the Jahn–Teller approach of Goodman,[10] the valence-shell-electron-pair-repulsion approach,[5–7,13,14] and a "pseudo-Jahn–Teller" molecular-orbital approach.

Goodman's conjecture was that since, in an O_h structure, there would be two electrons populating an antibonding a_{1g} molecular orbital, the energy to promote an electron would be modest. The usual appearance of various spectral features might be interpreted, then, on the basis of a very low-lying excited electronic state populated significantly at room temperature. Electronically excited molecules of O_h symmetry would presumably be in orbitally degenerate triplet states and hence would be subject to a Jahn–Teller deformation to a nondegenerate, distorted state.[43] The gaseous substance is not paramagnetic, however. A magnetic deflection molecular-beam experiment by Klemperer *et al.*[44] indicates that magnetic moments for XeF_6 molecules are only the order of nuclear magnetons. Magnetic properties of condensed phases of XeF_6 do not provide a check, among other reasons, because XeF_6 tends to associate in the liquid[45] and solid phases.[46] According to Goodman, zero-order symmetry considerations for the gaseous monomer require that a Jahn–Teller distortion preserve the center of symmetry and lead to a D_{4h} structure (by e_g deformation) or D_{3d} structure (by t_{2g} deformation). A D_{4h} structure shows no semblance of agreement with the experimental radial distribution curve, leading Goodman to favor a D_{3d}, O_h mixture. As stated in Sec. II, a D_{3d} model is compatible with the diffraction data provided a very large amplitude of vibration is assigned to the a_{2u} mode, even if no O_h molecules are assumed to be present. Therefore, the electron diffraction evidence cannot eliminate the model of Jahn–Teller deformation.

The theoretical model of Sidgwick and Powell[5] as augmented by Gillespie and Nyholm[6] and broadened later by Gillespie,[7] deserves special note. It correctly predicted the symmetrical structure of XeF_2 and XeF_4, as did several other theories but it was the only theory receiving wide attention which led to a prediction that XeF_6 would be distorted even in its nondegenerate ground state. According to the valence-shell–electron-pair-repulsion model, the Xe valence shell in XeF_6 contains eight Xe electrons and six F electrons for a total of seven pairs. Six pairs are considered to be bonding electron pairs attaching the ligands to the xenon atom. The remaining pair is taken as a localized sterochemically active lone pair. According to Gillespie's rules, a lone pair should occupy more space on the coordination sphere than a ligand, and should exert greater repulsions on neighboring pairs than does a bonding pair. These rules lead to quite clear and substantially corrent predictions concerning bond lengths and deformation angles for many molecules. On the basis of these rules we should, for example, expect a close similarity between XeF_6E (where E represents a lone pair) and IF_7. The most important prediction, perhaps, would concern which site on the coordination sphere corresponds to the site occupied by the lone pair. Since IF_7 appears to be a pentagonal bipyramid with longer and more crowded equatorial than axial bonds[15] (consistent with Gillespie's model), the spirit of Gillespie's rules would suggest that the "bulky" lone pair in XeF_6 occupy an axial site of a pentagonal bipyramid. Gillespie points out that high coordination numbers lead to added uncertainties in predicting geometries and he, himself, after learning of the smallness of deformation in XeF_6,[47] has favored the C_{3v} structure.[14] The present experiment, interpreted in terms of a nondegenerate ground state, relegates to the lone pair a markedly smaller region than that occupied by a ligand, in contradiction to Gillespie's rules.

Damaging as this failure of Gillespie's model appears at first glance, enough features of XeF_6 are accounted for by the valence-shell–electron-pair-repulsion model to justify continued interest in it. First of all, the model, almost alone, did predict an unusual structure. Second, the model predicted that bonds adjacent to the lone pair should be the longest bonds, a feature which is consistent with the diffraction findings. Gillespie[14] has suggested that the breakdown of his rule on lone-pair size is due to the fact that the "seven-coordinated" structure of XeF_6 is more crowded than lower coordinated structures which comply with his rules. While this rationalization is not without appeal, it should be noted that the shorter F–F distances (2.55 Å) in XeF_6 are significantly longer than those in SF_4[48] (2.21 and 2.39 Å) and ClF_3[49] (2.38 Å). These latter asymmetric molecules are more crowded than XeF_6 in this way of reckoning yet they follow the electron-pair-repulsion model.

The very simplicity of the reasonably successful Gillespie model—its absolute neglect of π bonding, of any details of s to p to d promotion energies, and of orbital overlap considerations—leads one to hope that a very simple valence-bond or molecular-orbital treatment might also give a similar spectrum of qualitative answers. To explore this possibility we set up the

[43] Provided spin–orbit coupling did not stabilize O_h symmetry. H. A. Jahn and E. Teller, Proc. Roy. Soc. (London) **A161**, 220 (1937). H. A. Jahn, *ibid.* **A164**, 117 (1938); **A168**, 469, 495 (1938).

[44] R. F. Code, W. E. Falconer, W. Klemperer, and I. Ozier, J. Chem. Phys. **47**, 4955 (1967).

[45] F. Schreiner, D. W. Osborne, J. G. Malm, and G. MacDonald, Chem. Eng. News **44**, 64 (1966).

[46] P. A. Agron, C. K. Johnson, and H. A. Levy, Inorg. Nucl. Chem. Letters **1**, 145 (1965).

[47] W. M. Tolles and W. D. Gwinn, J. Chem. Phys. **36**, 1119 (1962).

[48] D. F. Smith, J. Chem. Phys. **21**, 609 (1953).

[49] L. S. Bartell, R. M. Gavin, Jr., H. B. Thompson, and C. L. Chernick, J. Chem. Phys. **43**, 2547 (1965).

most elementary Hückel LCAO–MO model capable of being formulated with variable ligand electronegativity. It contained only enough atomic orbitals to house all of the electrons considered by Gillespie (s and p orbitals on Xe, and a p_σ orbital in each F). Nonbonded interactions were completely neglected; the only aspects of directed valence represented in the model were those of best effective chemical overlap consistent with the constraints of the Pauli exclusion principle. Details of the exact parameterization adopted to get numerical matrix elements for the secular equation are of no interest in the present experimental paper because the qualitative results we wish to stress were insensitive to these details. The simplest variant used is described elsewhere[50] and the most complex variant (in which, in some trials, xenon d orbitals were included) was essentially the Lipscomb–Lohr–Hoffmann method[51,52] stripped of nonbonded interactions. After completion of these calculations we learned of new, unpublished MO calculations by Lohr[53] for XeF_6 which include all Xe and F valence electrons and all nonbonded interactions. The variation of energy with geometry found by Lohr is virtually the same as that found by us.

The most surprising result of the MO model is its faithful mimicry of the Gillespie model in effects of lone pairs and ligand electronegativity in a series of four-, five-, six-, and seven-coordinated (including lone pairs) fluorides and methyl substituted fluorides.[54] It seems that both models capture certain topological invariants of quantum valence theory. Both models, however, overemphasize the tendency for XeF_6 to deform.

If the dependence of the molecular-orbital energy on geometry is expressed in terms of perturbation theory, some very useful deductions can be made on the basis of symmetry and these can be viewed as a partial rationalization of Gillespie's rules. Following Longuet-Higgins *et al.*[55] let us expand the Hamiltonian operator as a Taylor series.

$$H=H^0+H_i'S_i+\tfrac{1}{2}H_{ii}''S_i^2+\cdots, \qquad (33)$$

in the symmetry coordinate S_i for molecular deformation. An application of perturbation theory yields, for the ground electronic state, the result

$$E=E^0+\langle\psi_0\,|\,H_i'\,|\,\psi_0\rangle S_i+\{\tfrac{1}{2}\langle\psi_0\,|\,H_{ii}''\,|\,\psi_0\rangle$$
$$-\sum[\,|\,\langle\psi_0\,|\,H_i'\,|\,\psi_n\rangle\,|^2/(E_n-E_0)]\}S_i^2+\cdots. \qquad (34)$$

The first-order term is the Jahn–Teller term which vanishes for nondegenerate ground states. The second-order terms describe the force constant for S_i. We see at once that a small value of (E_m-E_0), coupled with a nonvanishing matrix element $\langle\psi_0\,|\,H_i'\,|\,\psi_m\rangle$, can lead to a low or even *negative* value of the force constant. When the mixing between ground and excited states on deformation is large enough to make a distortion energetically favorable (i.e., by making the force constant *negative*), the molecule is said to suffer a pseudo-Jahn–Teller effect. An examination of various molecular types shows that Gillespie deformations, as a rule, can be accounted for by this formalism.[56]

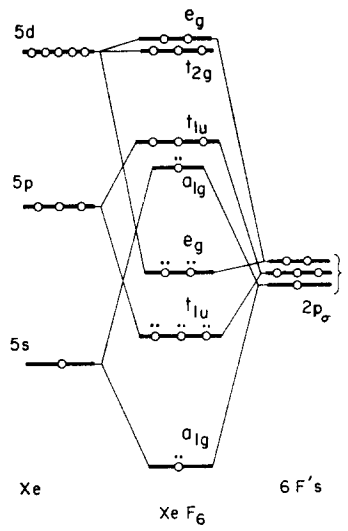

FIG. 8. XeF schematic correlation diagram illustrating MO energy levels for an O_h molecule.

Bader[57] has found that the lowest-lying excited state determines the characteristics of the force field, as a rule. If the ground-state wavefunction ψ_0 is totally symmetric, the matrix element $\langle\psi_0\,|\,H_i'\,|\,\psi_m\rangle$ will vanish unless H_i' has the same symmetry as ψ_m. The relevance of this to XeF_6 can be seen from the correlation diagram of Fig. 8. If the ground-state configuration is $(a_{1g}^*)^2$ [or for that matter, $(a_{1g}^*)(t_{1u}^*)$] the lowest excitation corresponds to $(E_{t_{1u}}-E_{a_{1g}})$, implying an especially low force constant for t_{1u} deformations. Such an interpretation accounts very well for the electron-diffraction result that t_{1u} amplitudes of vibration are enormous. It is also in accord with the fact that bond lengths near the lone pair tend to be longer than those away from the lone pair (by virtue of t_{1u} stretch $-t_{1u}$ bend "pseudo-Jahn–Teller interactions" lowering F_{34}.) It is not in accord with Willett's suggestion[58] that d-orbital involvement is what destabilizes O_h symmetry for XeF_6. The excitation energy $(E_{t_{2g}}-E_{a_{1g}})$ must be much greater than $(E_{t_{1u}}-E_{a_{1g}})$, and the d involvement would correspond to t_{2g} defor-

[50] L. S. Bartell, Inorg. Chem. **5**, 1635 (1966).
[51] L. L. Lohr, Jr., and W. N. Lipscomb, Ref. 1, p. 347.
[52] R. Hoffmann, J. Chem. Phys. **39**, 1397 (1963).
[53] L. L. Lohr, Bull. Am. Phys. Soc. **12**, 295 (1967).
[54] R. M. Gavin, Jr., and L. S. Bartell (unpublished).
[55] U. Öpik and M. H. L. Pryce, Proc. Roy. Soc. (London) **A238**, 425 (1957); D. H. W. DenBoer, P. C. DenBoer, and H. C. Longuet-Higgins, Mol. Phys. **5**, 387 (1962); B. J. Nicholson and H. C. Longuet-Higgins, *ibid.* **9**, 461 (1965).
[56] L. S. Bartell, Symposium on Models for Discussion of Molecular Geometry, American Chemical Society Meeting, Chicago, Ill., September 1967; J. Chem. Educ. (to be published).
[57] R. F. W. Bader, Mol. Phys. **3**, 137 (1960).
[58] R. D. Willett, Theoret. Chim. Acta **6**, 186 (1966).

mations. Numerical calculations[53,54] support the minor importance of the *second-order* t_{2g} term in comparison with the t_{1u} term.

The essential difference between XeF_2 and XeF_4, which are symmetrical, and XeF_6, which tends to distort, would seem to be the steadily rising energy of the antibonding a_{1g} MO as the number of antibonding ligand interactions goes up. This would decrease the lowest-lying (E_m-E_0) and enhance the pseudo-Jahn–Teller interaction. That the pseudo-Jahn–Teller effect is related to the Gillespie lone pair is easily seen. If, for XeF_6, the pair $(a_{1g}^*)^2$ is removed, the lowlying $t_{1u}^*\leftarrow a_{1g}^*$ transition no longer exists and the pseudo-Jahn–Teller situation vanishes. The resultant system is isoelectronic with TeF_6 which is known to be a regular octahedron[12] with a t_{1u} force constant[59] nearly two orders of magnitude higher than the highest alternative deduced for XeF_6 in Sec. IV.

It is instructive to check our conclusions on lone-pair influence and site preference by analogy with other molecules. In the formalism of this section, XeF_6 differs from TeF_6 (O_h) in the $t_{1u}^*\leftarrow a_{1g}^*$ transition which lowers the XeF_6 quadratic constant, F_{44}. The large t_{1u} displacement then makes V_{445} (the relevant pure bend term of steric form) important, tending to stabilize a C_{3v} structure with the lone pair in the *face* of the octahedron. Similarly, SF_4 differs from SiF_4 (T_d) in having a low-lying $t_2^*\leftarrow a_1^*$ transition which lowers the SF_4 t_2 quadratic constant, F_{44}. The large t_2 displacement then makes V_{442} (the relevant pure bend term of steric form) important, tending to localize the lone pair at the minimum of $(V_{44}+V_{442})$. For SF_4, the minimum of this function is easily seen to be at the *edge* of the reference tetrahedron, in agreement with experiment,[48] instead of in the face. Accordingly, SF_4 has C_{2v} symmetry instead of C_{3v}. An analogous argument applied to ClF_3 in its deformation[49] from the D_{3h} symmetry of BF_3.

VII. COMPARISON WITH ISOELECTRONIC IONS

The ICl_2^- and ICl_4^- anions which guided chemists in predictions of the structures of XeF_2 and XeF_4 may have led to the correct results for partly wrong reasons. Parallel reasoning based on the known[60] O_h structures of $(TeCl_6)^{2-}$, $(TeBr_6)^{2-}$, and $(SbBr_6)^{3-}$ would have suggested that the isoelectronic molecule XeF_6 is a regular octahedron. Conversely, the application of Gillespie's rule to the tellurium and antimony ions would have led (and originally, *did* lead)[6] to a prediction of distortion from O_h symmetry. Gillespie and others have rationalized this breakdown of the Gillespie rules on the basis of the difficulty in packing so many bulky chloride or bromide ions into the coordination sphere. Sundry other explanations such as interionic forces have been advanced but the plausibility of the steric argument is borne out by an empirically calibrated coordination number rule formulated by Rundle[61] before XeF_6 was known. According to Rundle's scheme, for example, 7.1 fluorines but only 5.6 chlorines could be accommodated in the cordination sphere of xenon. The gaseous ion IF_6^- would be less subject to steric resistance to t_{1u} deformations than the other ions listed above and, presumably, would have structural characteristics similar to those of XeF_6. It may be noted, however, that certain diffraction phase relationships surviving in electron-diffraction studies of gaseous monomers are lost in x-ray diffraction studies of crystalline arrays. Accordingly, if XeF_6 units in crystals were executing the same vibrations as we propose for the dynamic model of freely inverting, non-O_h molecules, the x-ray patterns would detect O_h units with only slightly large thermal amplitudes. Nothing about the unusual correlation between t_{1u} and t_{2g} modes would be revealed. Similarly, asymmetric fields in the crystal might very easily freeze the ion into "statically deformed" units such as are discussed in Sec. II. Moreover, if the deformed ions were distributed in randomly disordered arrays, the x-ray method would disclose only apparently O_h structures. Therefore the information derived from crystallographic studies of ions ieoelectronic with XeF_6 must be interpreted with caution.

VIII. CONCLUSIONS

Vapor-phase electron-diffraction patterns show that xenon hexafluoride is an approximately octahedral molecule exhibiting large amplitudes of bending vibrations. Diffracted intensities cannot be accounted for, however, by an O_h molecule vibrating in *independent, uncorrelated* normal modes. The abnormal breadth of the Xe–F distribution indicates that, over a time scale of many stretching vibrations, the molecule contains nonequivalent bonds (mean length, 1.890±0.005 Å). The F–F nonbonded distribution function reveals that the molecule oscillates predominantly in the broad vicinity of C_{3v} configurations. These configurations are characterized by substantial t_{1u} and t_{2g} deformations correlated in phase, and express the tendency of ligands to avoid one site on the coordination sphere (perhaps the site of a "stereochemically active lone pair"). Of the two large deformations, at least the t_{1u} mode is undergoing large amplitudes of vibration.

Although the diffraction data do not disclose the three-dimensional characteristics of the molecular geometry in full detail, they do restrict the possibilities to a small number of alternatives, assuming that the gas molecules exist in a single electronic state. Notwith-

[59] G. Nagarajan, Bull. Soc. Chem. Belg. **71**, 674 (1962).

[60] G. Engel, Z. Krist. **90**, 341 (1935); E. E. Aynsley and A. C. Hazell, Chem. Ind. (London) **1963**, 611; I. D. Brown, Can. J. Chem. **42**, 2758 (1964); S. Lawton and R. Jacobson (private communication, 1965).

[61] R. E. Rundle, Record Chem. Progr. (Kresge-Hooker Sci. Lib.) **23**, 195 (1962). A slight modification in the scheme is introduced by R. E. Rundle, Survey Progr. Chem. **1**, 81 (1963).

standing the small fraction of the time that XeF_6 spends near O_h symmetry, it appears to be possible to construct a molecular potential-energy function more or less compatible with the diffraction data in which the minimum energy occurs at O_h symmetry. The most notable feature of this model is the almost vanishing restoring force for small t_{1u} bending distortions. Indeed, the mean curvature of the potential surface for this model corresponds to a ν_4 force constant of 10^{-2} mdyn/Å or less. Various rapidly inverting non-O_h structures embodying particular conbinations of t_{2g} and t_{1u} deformations from O_h symmetry give equally acceptable radial functions, however. Distributions of configurations joining the eight equivalent C_{3v} structures of Sec. II via low-barrier pathways through C_{2v} intermediates give the best agreement with experiment obtained to date. In the region of molecular configuration where the gas molecules spend most of their time, the form of the potential-energy function required to represent the data does not distinguish between a Jahn–Teller first-order term or a cubic V_{445} term as the agent responsible for introducing the t_{2g} deformation. The Jahn–Teller term is consistent with Goodman's interpretation of the molecule. On the other hand, the cubic term is found to be exactly analogous to that for other molecules with stereochemically active lone pairs (e.g., SF_4, ClF_3).

For all of the above alternatives the *most probable* configuration is the same ($\approx C_{3v}$), and the subtleties in the time weighting of instantaneous structures will not be established until a careful spectroscopic characterization of the molecular force field is available. The diffraction data seem to be accounted for adequately without invoking a Jahn–Teller effect, although an analysis of the data in which the implied unconventional intramolecular motions are handled in a fully rigorous manner has not yet been carried out.[62] Weighing against the Jahn–Teller interpretation is the apparent absence of paramagnetism in the gas phase.[44]

One noteworthy finding is the failure of XeF_6 to conform to the static deformation limit required by the popular valence-shell–electron–pair-repulsion model of Gillespie *et al.*,[5–7] although some of the predicted structural features are observed. Of special interest is the applicability of the formalism of the pseudo-Jahn–Teller effect (see Sec. VI) which seems to provide a rationale for the main rules of the Gillespie model and accounts, in the present case, for the very low t_{1u} bending force constant. We must not be too dogmatic about the detailed failure of the model of Gillespie *et al.* in a higher coordination case than the model has been calibrated for. The singlet-state model at greatest variance with Gillespie's rules is the O_h equilibrium model. Even if *this* model proves to be the correct one, the failure of the pair-repulsion model is only a small one in the following sense. It would seem more or less accidental, viewed in terms of the pseudo-Jahn–Teller lowering of the F_{44} force constant from, say, 0.8 mdyn/Å (its value for TeF_6)[59] to 0.01 mdyn/Å or less, that the force constant stopped short of going appreciably negative. A value of perhaps -0.1 mdyn/Å would suffice to make the deformation essentially static.

Irrespective of the uncertainty in the detailed shape of the potential-energy function, we can conclude that XeF_6 is an exceptionally flexible molecule with an equilibrium structure at most a modest distance from O_h symmetry. Its anomalous properties are undoubtedly related to its exceedingly low restoring force for a t_{1u} deformation.

Note added in proof: In the structure analysis of Sec. III the coupling between t_{1u} and t_{2g} modes was taken crudely into account, but an analysis in which molecular configurations were weighted to be fully self-consistent with the potential energy perturbation was not attempted. This deficiency has now been remedied, as promised in Ref. 62. The leading anharmonic constant F_{445} has been found to be of the magnitude suggested by Eq. (24). Discouraging a detailed analysis is the fact that quartic and higher terms in the potential energy appear to be significant. The diffraction data contain insufficient information to establish these terms. The best fit of the diffraction data occurs when the potential function exhibits double minima along the t_{1u} bending coordinates, corresponding to an equilibrium structure at C_{3v} symmetry (i.e., somewhat to the right of the free-rotator model of Fig. 7). Consistent with this interpretation is a new infrared study of XeF_6 in an argon matrix at liquid helium temperatures.[63] In the ground vibrational state, XeF_6 exhibits C_{3v} selection rules. The temperature dependency of excited states is interpreted in terms of the free-rotator model with $\nu_{01}\approx 7\pm 5$ cm^{-1}, in agreement with the electron diffraction prediction for this model of ≈ 10 cm^{-1}.[36]

ACKNOWLEDGMENTS

In our analyses we have profitted from conversations with many colleagues including, especially, Dr. H. B. Thompson and Dr. C. Nordman. We are particularly indebted to Dr. Brian Nicholson for pointing out the relevance of the pseudo-Jahn–Teller formalism and to Dr. K. Kuchitsu for carrying out the calculations summarized in the note added in proof.

[62] A treatment in which the weighting of configurations is consistent with the potential function coupling the modes is in progress.

[63] H. Kim, Bull. Am. Phys. Soc. **13**, 425 (1968).